# A Binned Approach to Cloud-Droplet Riming Implemented in a Bulk Microphysics Model

STEPHEN M. SALEEBY AND WILLIAM R. COTTON

*Colorado State University, Fort Collins, Colorado*

(Manuscript received 5 December 2006, in final form 26 April 2007)

ABSTRACT

This paper presents the development and application of a binned approach to cloud-droplet riming within a bulk microphysics model. This approach provides a more realistic representation of collision–coalescence that occurs between ice and cloud particles of various sizes. The binned approach allows the application of specific collection efficiencies, within the stochastic collection equation, for individual size bins of droplets and ice particles; this is in sharp contrast to the bulk approach that uses a single collection efficiency to describe the growth of a distribution of an ice species by collecting cloud droplets. Simulations of a winter orographic cloud event reveal a reduction in riming when using the binned riming approach and, subsequently, larger amounts of supercooled liquid water within the orographic cloud.

## 1. Introduction

Mixed-phase clouds, consisting of both frozen hydrometeors and supercooled liquid water, commonly exist in wintertime snowfall events over the western United States. Generally, much of the condensate is produced by large-scale synoptic lifting. However, over the mountainous terrain of Colorado, the additional production of condensate (supercooled cloud droplets) near mountaintop is enhanced by orographic lifting (Rauber and Grant 1986). Subfreezing orographic clouds may act as a region of snow crystal growth via riming of supercooled droplets (Borys et al. 2000, 2003). This orographically enhanced snow growth process has been termed the "seeder–feeder" couplet (Reinking et al. 2000). In this process, unrimed snow crystals falling from mid- to upper-level "seeder" clouds must descend through the "feeder" cloud of supercooled droplets before reaching the surface. The region of the heaviest riming has been shown to occur in the lower levels within 1–2 km of the surface (Rauber et al. 1986; Heggli and Rauber 1988; Warburton and DeFelice 1986). This low-level riming process enhances the precipitation efficiency, such that the amount of rime has been shown to comprise up to 20%–50% of the final snow mass that reaches the surface (Mitchell et al. 1990; Borys et al. 2003). Enhanced riming will increase the mass of snow crystals as well as the fall speed; this increases the likelihood of higher snow deposits along windward slopes (Hindman 1986). Slower-falling, unrimed snow crystals are more likely to fall on the leeward slopes where subsidence leads to evaporation, a reduction in surface snowfall, and disappearance of the feeder cloud (Rauber and Grant 1986). Dry-season water supplies in Colorado rely strongly on the winter snowpack, which is quite dependent upon riming to enhance precipitation efficiency.

Forecasters and hydrologists rely upon numerical weather prediction models to aid in the prediction of snowfall and the melt-season runoff for estimation of streamflow. The Regional Atmospheric Modeling System (RAMS) has been utilized as a real-time forecast model at Colorado State University since 1991 (Cotton et al. 1994). This has spawned collaborative efforts with National Weather Service offices at Grand Junction, Colorado, Pueblo, Colorado, and Cheyenne, Wyoming (McAnelly et al. 2000). RAMS has also been demonstrated as an excellent research tool for mesoscale modeling of winter events (Poulos et al. 2002; Meyers et al. 2003; Saleeby and Cotton 2005). The distinguishing factor for using RAMS to simulate winter events is its microphysics package (Walko et al. 1995; Meyers et al. 1997; Cotton et al. 2003; Saleeby and Cotton 2004). This

*Corresponding author address:* Stephen M. Saleeby, Department of Atmospheric Science, Colorado State University, Fort Collins, CO 80523.
E-mail: smsaleeb@atmos.colostate.edu

DOI: 10.1175/2007JAMC1664.1

is essential for realistically representing mixed-phased cloud processes in winter events. Currently, RAMS microphysics is run efficiently and timely as a bulk model, whereby the hydrometeor distributions are represented by the gamma function,

$$n(D) = \frac{N_t}{\Gamma(\nu)} \left(\frac{D}{D_n}\right)^{\nu-1} \frac{1}{D_n} \exp\left(-\frac{D}{D_n}\right), \qquad (1)$$

where $n(D)$ is the number of hydrometeors of diameter $D$, $N_t$ is the total number, $\nu$ is the shape parameter, and $D_n$ is the characteristic diameter of the distribution. RAMS predicts the mixing ratio and number concentration of cloud droplets, rain, pristine ice, snow, aggregates, graupel, and hail, while specifying a certain shape parameter of the distributions. Saleeby and Cotton (2004) introduced a two-mode distribution of cloud droplets characterized by small and large cloud-droplet modes. These are named cloud1 and cloud2, and they have diameters that range from 0 to 40 and from 40 to 80 $\mu$m, respectively. This two-mode representation serves to better represent the full droplet spectrum as is often observed in nature (Hobbs et al. 1980).

Given the relative importance of riming on snowfall, it is important that the collision–coalescence processes be simulated as accurately as possible. As is commonly practiced in bulk microphysics models, the riming approach in RAMS makes use of the bulk distributions of the hydrometeors. The stochastic collection equation of Verlinde et al. (1990) and Walko et al. (1995) is applied for the collection of cloud droplets by each of the ice species, except for pristine ice, whose collection rates for cloud droplets have been found to be negligible at sizes less than a couple of hundred microns. The collection equation for mixing ratio, from Walko et al. (1995), is given as

$$\frac{dr_x}{dt} = \frac{N_{tx} N_{ty} \pi F_\rho}{4\rho_a} \int_0^\infty \int_0^\infty m(D_x)(D_x + D_y)^2 |\upsilon_{tx}(D_x) - \upsilon_{ty}(D_y)| f_{\text{gam}x}(D_x) f_{\text{gam}y}(D_y) E(x, y)\, dD_x\, dD_y, \qquad (2)$$

where $r$ is the mixing ratio, $N_t$ is the number concentration, $m$ is the mass, $\upsilon_t$ is the fall velocity, $E$ is the collection efficiency, $D$ is the diameter, $\rho_a$ is air density, $f_{\text{gam}}$ is the gamma distribution, $F$ is a density-weighting factor for collection at different elevations, $x$ is the collected species, and $y$ is the collector species. A similar approach is applied to number concentration and is discussed in Meyers et al. (1997). While this method is certainly viable for a bulk model, one particular shortcoming is the use of a single collection efficiency for an entire distribution of cloud droplets and a given ice species. Previously in RAMS, the bulk computation of riming efficiency for snow and aggregates was determined from empirical relationships to be

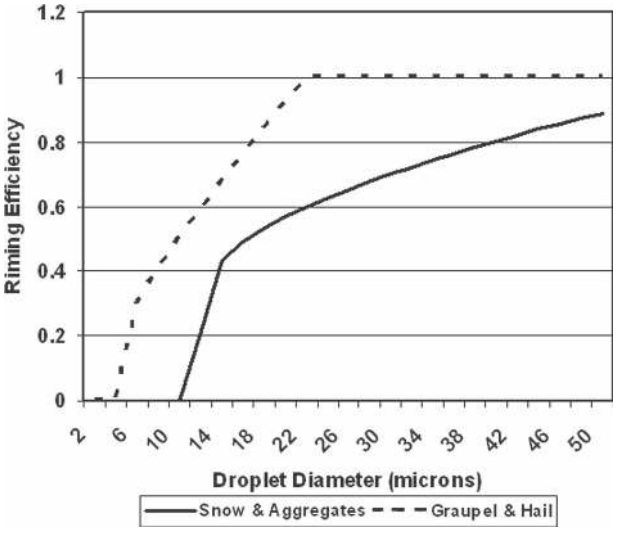


FIG. 1. Plots of collection efficiency used by RAMS bulk riming scheme in the computation of cloud-droplet riming by the ice species.

$$E(x, y) = 30(\overline{m}_{\text{cloud}} - 9.0 \times 10^{-13})^{0.15}, \qquad (3)$$

where $\overline{m}_{\text{cloud}}$ is the mean mass (kg) of the cloud-droplet distribution, and $E$ must be no more than 1. For riming by graupel and hail, the efficiency was

$$E(x, y) = 1426(\overline{m}_{\text{cloud}} - 3.4 \times 10^{-14})^{0.28}. \qquad (4)$$

For both equations, the mean mass is computed from the mixing ratio and number concentration. The mean mass is related to diameter via power-law relations, which are discussed in the following section. Plots of the bulk collection efficiency curves are shown in Fig. 1. These riming efficiencies are solely dependent upon droplet mean mass–diameter. The impact of ice hydrometeor mean diameter is built into the solutions of the stochastic collection equation.

The identification of the importance of riming upon accumulated snowfall in Colorado and other semiarid mountainous western states, suggests the need for a more representative approach to riming, with collection efficiencies that vary with sizes of ice particles and cloud droplets. Thus, a quasi-binned riming approach was developed to more realistically represent riming across the distributions of supercooled cloud droplets and ice species.

## 2. Description of binned riming approach

The following section describes the details of the binning approach to riming. This binning method is differ-

ent from traditional bin microphysics in that we do not perform explicit computations for riming within each bin for application to predictive equations for each bin. Rather, we take the bulk hydrometeor gamma distributions and temporarily divide them into a number of separate bins. The division into bins will vary with mixing ratio and mean diameter of the hydrometeors. Thus, for a range of mixing ratios and mean diameters, the gamma curves are binned, computations are run for all bin interactions, and the curve is essentially reconstructed, or summed, to give the total riming that would occur. Even though the shape of the hydrometeor distribution remains constant, we can gain more accuracy by allowing hydrometers of different sizes to interact with truly applicable collection efficiencies for the specific bin sizes. In contrast, a typical bulk approach uses the same gamma distribution as a binning approach, but applies a single average collection efficiency to represent the whole size distribution. The details of the method follow hereafter.

The binning method in RAMS utilizes the method-of-moments scheme (Tzivion et al. 1987; Cotton et al. 2003) that is currently applied for cloud-droplet autoconversion and collection of cloud droplets by rain. This method allows for riming of both the cloud1 and cloud2 modes by each ice species (snow, aggregates, graupel, and hail). To simplify the following parameterization description, only riming by snow will be addressed. The same method, however, is applied for each ice species with appropriately applied mass–diameter and fall velocity–diameter power laws. The power laws (in mks units) take the form $m = c_m D^{p_m}$ and $\upsilon = c_\upsilon D^{p_\upsilon}$, where $m$ is mass, $c_m$ and $c_\upsilon$ are the mass coefficients, $\upsilon$ is fall velocity, and $p_m$ and $p_\upsilon$ are the power coefficients.

This riming parameterization uses a lookup table approach to determine the amount of cloud water that is collected by snow. The lookup tables provide the rime amount based upon the mean diameter of cloud droplets, mean diameter of snow, mixing ratio of snow, number concentration of cloud droplets, and the time-step length. The rimed amount is computed from the method of moments as described by Tzivion et al. (1987). The method of moments, formerly applied to RAMS for liquid cloud water autoconversion, uses a 36 mass-doubling bin approach for liquid droplets beginning with a minimum droplet size of ~3 $\mu$m. Bins 1–15 contain droplet sizes in the cloud water range (<80 $\mu$m). Thus, any sizes larger than 80 $\mu$m are given to the rain category. This hydrometeor bin sizing and method of moments was then adapted for snow-collecting cloud droplets by replacing the rain-sized bins with snow in those bins. Appropriate mass–diameter power laws for snow were used because mass doubling varies with the type–density of hydrometeors.

The method of moments, used to compute the collected mass of cloud droplets, is hydrometeor dependent in the calculation of the hydrodynamic kernel, which for liquid hydrometeors is given as

$$K(r_1, r_2) = E_c \pi (r_1 + r_2)^2 |V_1 - V_2|, \tag{5}$$

where $K$ is the collection kernel, $r_1$ and $r_2$ are the radii of two colliding liquid droplets, and $V_1$ and $V_2$ are the fall velocity of the respective droplets. The approach discussed in Tzivion et al. (1987), however, uses a mass-based, rather than radius-based, collection kernel for the collection computations. With some algebraic computations, this can be derived as

$$K(x, y) = \left(\frac{9}{16}\pi\right)^{(1/3)} (x^{1/3} + y^{1/3})^2 E_c(x, y) |V_x - V_y|, \tag{6}$$

where $x$ and $y$ represent the mass of the respective colliding droplets (this equation is in cgs units). To apply this to cloud droplets being collected by snow, we cannot assume that the mass–diameter relation for spherical liquid droplets applies for snow. Thus, we use specific power-law equations from RAMS that relate snow mass to diameter and snow velocity to diameter. Again, algebraic manipulation and conversion between RAMS power laws in mks units to the hydrodynamic kernel in cgs units gives us the final collection kernel equation for snow to be used by the method of moments:

$$K(x, y) = \pi \left\{ \left(\frac{3}{4}\frac{x}{\pi}\right)^{1/3} + 50 \left[ \frac{y}{1000} \frac{1}{(2.739e^{-3})} \right]^{1/1.74} \right\}^2 \times E_c(x, y) |V_x - V_y|, \tag{7}$$

where the snow mass power-law equation in mks units is $m = 2.739e^{-3} D^{1.74}$. The velocity power law ($V = 27.7 D^{0.484}$; mks units) for snow is likewise used for the fall velocity component of the hydrodynamic kernel.

It should be noted that hydrometeor power-law relationships for the mass and velocity of snow are applied for all realistic diameters. The power laws are most appropriate for unrimed snow, but they do account for changes in mass–fall velocity resulting from diameter changes imposed by light riming. In the case of heavy riming, it is likely that a snow crystal would increase greatly in density while only experiencing a minor change in diameter. This would tend to increase the fall speed in a manner that the power laws cannot simulate. However, in the case of heavy riming, the snow would be subsequently transferred to the graupel category, such that the graupel power laws would apply thereafter.

Perhaps the most crucial and unique aspect of using binned riming is the application of unique collection efficiencies applied to the interaction of all snow size bins with all cloud-droplet size bins. This is much more representative of the true efficiency of the riming process when compared to the single collection efficiency applied over the full range of distribution sizes of snow and cloud droplets in a bulk microphysics collection method. As such, we have selected collection efficiencies documented in the literature for riming by snow, aggregates, graupel, and hail. The collection efficiencies used for snow and aggregates come from Wang and Ji (2000). We apply the efficiencies (from their Fig. 8) to represent snow columns; a matrix of efficiency values are fed into the hydrodynamic kernel solver to determine the kernel values for riming interactions of all cloud-droplet-sized bins with all snow crystal–sized bins.

The representation of aggregates is a more difficult matter because these are poorly understood and can take many forms. Lew et al. (1986a,b) have shown that there is great variability in the degree of riming, the riming efficiencies, and collection kernels for aggregates due to possible variations in the porosity. The porosity can vary substantially, depending on the types of snow crystals that comprise the aggregates. As such, there are no reliable, generalized sets of collection efficiencies available to apply to aggregate riming. They did show, however, that the riming efficiency of porous aggregates tended to be greater than that of individual crystals. Given this dilemma, we decided to use the collection efficiences for hexagonal plates to compute the collection of droplets by aggregates. The hexagonal plates, discussed in Wang and Ji (2000), tend to have a large surface area for riming and relatively high collection efficiencies, which may reasonably represent the large surface area for riming on aggregates of crystals. As aggregates become better understood, and more representative collection efficiencies become available via observations or laboratory studies, this parameterization can be updated and further tested. For now, we believe that this representation of aggregate collection efficiencies provides a step toward improvement of simulating their growth by riming.

Graupel and hail collection efficiencies were computed from the work of Cober and List (1993) and Greenan and List (1995), respectively. The equation for graupel efficiencies is given as $E = 0.55 \log(2.51K)$. Here, $K$ is the Stokes parameter given as $K = (2\rho_d V r_d^2)/(9\eta r_t)$, where $\rho_d$ is the droplet density, $V$ is the relative velocity between the cloud droplet and collector, $r_d$ is the droplet radius, $r_t$ is the collector radius, and $\eta$ is the dynamic viscosity of air. For hail, the computation is given as $E = 0.59K^{0.15}$, where, again, $K$ is the Stokes parameter. Sample collection curves for each ice species collecting cloud droplets in this binned parameterization are given in Fig. 2. These collection curves are given for a single ice hydrometeor size of 1 mm, though they are allowed to vary across a broad range of ice crystal diameters when solving the hydrodynamic kernel.

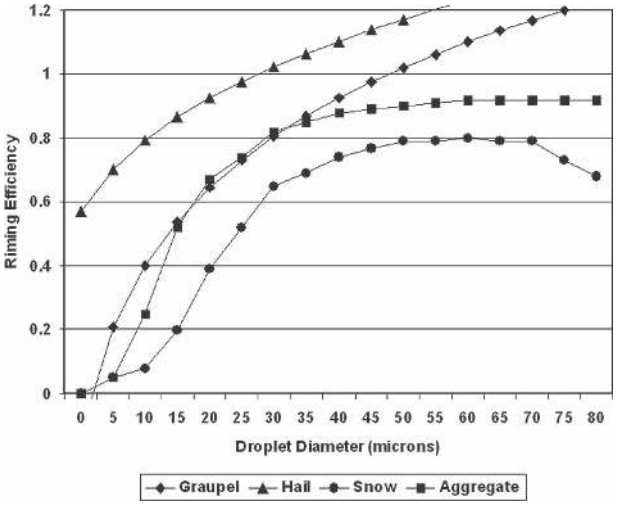


FIG. 2. Plots of collection efficiency used by RAMS binned riming scheme in the computation of cloud-droplet riming by the ice species with a diameter of 1 mm.

To summarize, the documented collection efficiencies for collisions of cloud droplets with snow were supplied to the functions for the computation of the collection kernel over all reasonable size ranges of droplets and snow crystals. The collection kernels were then fed into the computation of the method of moments to determine the amount of cloud water rimed by snow when considering the collisions of all droplet sizes with all snow crystal sizes. This determines the total cloud water that is removed and collected by snow.

The addition of liquid to the surface of ice particles impacts the thermal characteristics of the ice. Thus, following the approach of Walko et al. (1995), we compute the thermal energy of the coalesced cloud and ice mixing ratios as $Q^* = (Q_i \Delta r_i + Q_L \Delta r_L)/r^*$. Here, $Q_i$ and $Q_L$ are the thermal energies of coalesced ice and liquid, respectively, $r_i$ and $r_L$ are the mixing ratios of coalesced ice and liquid, respectively, and $r^*$ is the total coalesced mixing ratio. The thermal energy is used to compute the portions of coalesced mass that are liquid and ice. If the collecting species is snow or aggregates, any liquid-droplet mass or melted ice mass is transferred to the graupel category; if the rimed mass freezes upon impact, the mass is added to snow or aggregates. (We specify snow and aggregates to be completely frozen.) If graupel rimes cloud water and then freezes, the rimed mass remains with graupel. However, if the rimed mass

remains liquid or causes the coalesced graupel to melt, part of the liquid is transferred to hail and part remains with graupel, because graupel is allowed to have a wetted surface. All cloud water rimed by hail remains with the hail category. At this point in the computations, riming is complete. Following this process, the hydrometeor thermodynamic subroutines in RAMS will determine whether further shedding of liquid from graupel or hail should occur.

## 3. Test simulations

The winter case study used for testing the binned riming scheme is the same as that discussed in Saleeby and Cotton (2005), from 28 to 29 February 2004. This winter event over the mountains of Colorado began producing snowfall at the Storm Peak Laboratory (SPL) around 1200 UTC 28 February and continued through at least 1500 UTC 29 February. SPL sits atop the western end of the summit of Mt. Werner (~3210 m MSL) at the Steamboat Springs Ski Resort just east of the town of Steamboat Springs, Colorado. SPL is run by the Desert Research Institute and it houses a sophisticated cloud microphysics and aerosol measurement laboratory (Borys and Wetzel 1997). A primary appeal of SPL is that during the winter months, the laboratory sits within an orographic cloud ~25% of the time (Borys and Wetzel 1997). The orographic cloud generally forms under conditions of northwesterly flow as wintertime baroclinic low pressure systems propagate toward Colorado from the Pacific Northwest.

The RAMS model simulations were configured with multiple nested grids roughly centered over the Steamboat Springs area. Model grids 1, 2, and 3 had gridpoint spacings of 50, 10, and 2 km, respectively, whereby subsequent grids were nested within the previous grid (see Fig. 3). The minimum vertical spacing was set to 100 m, with a stretch ratio of 1.1 and a maximum spacing of 800 m at the highest vertical levels. The 6-hourly North American Regional Reanalysis was utilized for model initial conditions and lateral boundary nudging, with lateral nudging on the parent grid occurring at a 15-min time scale. The model also made use of the two-moment microphysics package (Meyers et al. 1997); a two-stream, hydrometeor-sensitive radiation scheme (Harrington 1997); and the Kain–Fritsch cumulus parameterization on the outermost grid (Kain and Fritsch 1993).

Simulations were initialized with a cloud condensation nuclei (CCN) concentration of 200 $cm^{-3}$ and giant-CCN concentration of $10^{-3}$ $cm^{-3}$, whereby the activation of nuclei was determined by the degree of supersaturation induced by vertical motion (Saleeby and Cotton 2004). During this event the highest cloud-droplet concentration reached approximately 140 $cm^{-3}$, and was thus representative of a relatively clean air mass with little mountaintop contamination from valley pollution. As such, we chose to initialize the model with a homogeneous field of CCN of relatively low concentration. For the testing of this binned riming approach, the choice of aerosol concentrations for initialization is important but somewhat arbitrary because no measurements are available; but, given that our focus here is to compare the impacts of the binned versus bulk riming schemes, this approach is reasonable.

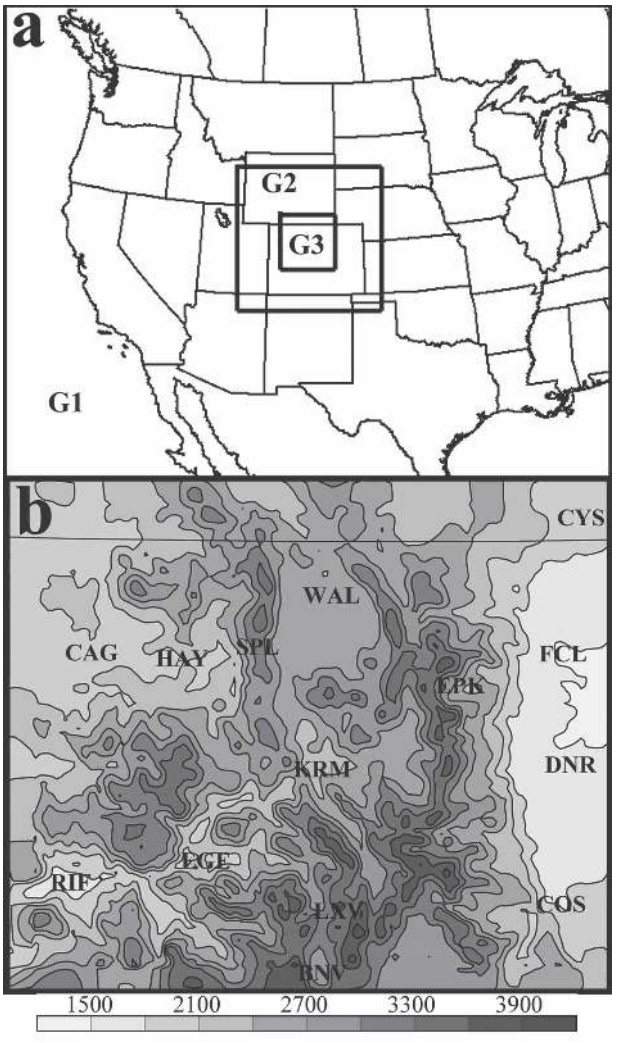


FIG. 3. Grid configuration for riming scheme test cases: (a) three-nested-grid setup, with grids 1, 2, and 3 denoted by the labels G1, G2, and G3; and (b) a zoomed-in view of grid 3 with 2-km grid spacing. The topography (m) and selected city identifiers are overlaid.

Between 1200 UTC 28 February and 1500 UTC 29 February 2004, 27 mm of liquid-equivalent precipitation was recorded at the Steamboat Springs Patrol Headquarters, and the RAMS model predicted nearly

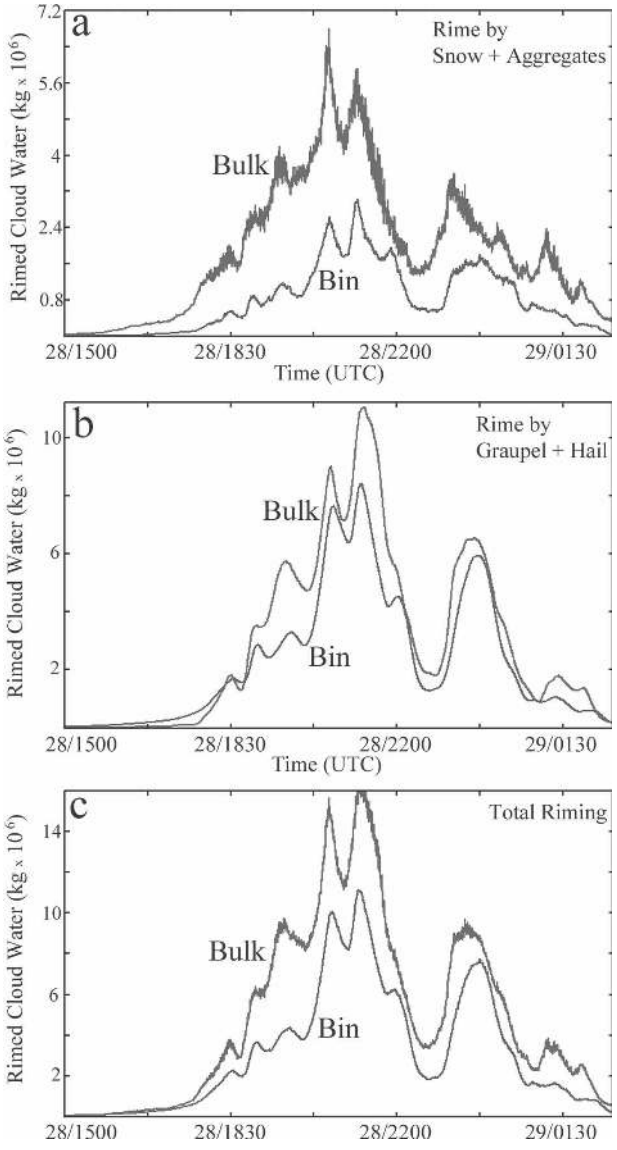


FIG. 4. Time series of domain-summed rimed cloud water mass by (a) snow and aggregates, (b) graupel and hail, and (c) all ice species combined. Snow and aggregates are ice-only species, and graupel and hail can both be partially liquid. The curves labeled "Bulk" and "Bin" used the bulk and binned riming schemes, respectively.

the same (see Saleeby and Cotton 2005). Periodic measurements of cloud-droplet liquid water content and droplet concentration were made on the SPL observation deck with the use of a Particle Measuring Systems, Inc., (PMS) Forward Scattering Spectrometer Probe (FSSP)-100 (Borys et al. 2000). Comparisons between the RAMS-predicted cloud water and measured cloud water at SPL will help to provide validation and a level of confidence in the application of the developed binned riming module. See Saleeby and Cotton (2005) for greater details of the snowfall event.

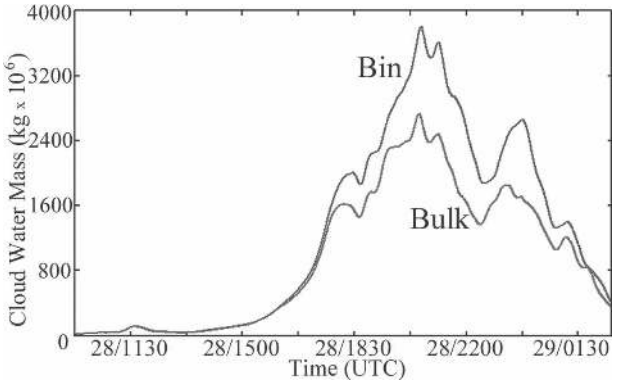


FIG. 5. Time series of the domain-summed mass of cloud water. The curves labeled "Bulk" and "Bin" used the bulk and binned riming schemes, respectively.

## 4. Module intercomparison

The use of specific collection efficiencies in the computation of cloud-droplet riming certainly provides a more realistic solution than the bulk approach for this microphysical growth process. Comparative simulations, in which riming is known to play a substantial role, should therefore provide a reduction of previous biases that were present by using an oversimplified approach (Cotton et al. 2006). Prior to this work, it was speculated by Cotton et al. (2006) that RAMS was overdepleting cloud water in many, but not all, cases that have been examined. This suspicion of overriming is what provided motivation to develop this new approach in RAMS.

The forthcoming comparative figures are taken from results of the innermost nested grid with 2-km grid spacing, which covers much of the Colorado high terrain (see Fig. 3). Figure 4 depicts the time series of domain-summed rimed mass from grid 3 for the riming by snow and aggregates combined (ice only), graupel and hail combined (which can be mixed phased), and for all ice species together. In each panel and at nearly all times, the use of the binned riming method reduced the degree of riming of cloud droplets within the model domain as a whole. This suggests that use of a single value for collection efficiency, based solely on the mean mass of the distribution, tends to overpredict the amount of riming that takes place. Furthermore, the amount of cloud water that is present subsequently responded to the reduced riming. The time series of domain-summed cloud water mass is shown in Fig. 5. The reduced riming resulted in the presence of more cloud water for the duration of the simulation. The greatest difference in cloud water mass, between the bulk and bin method, corresponds to the timing in the occurrence of the greatest difference in the amount of riming. Likewise, when the difference in rimed amounts is

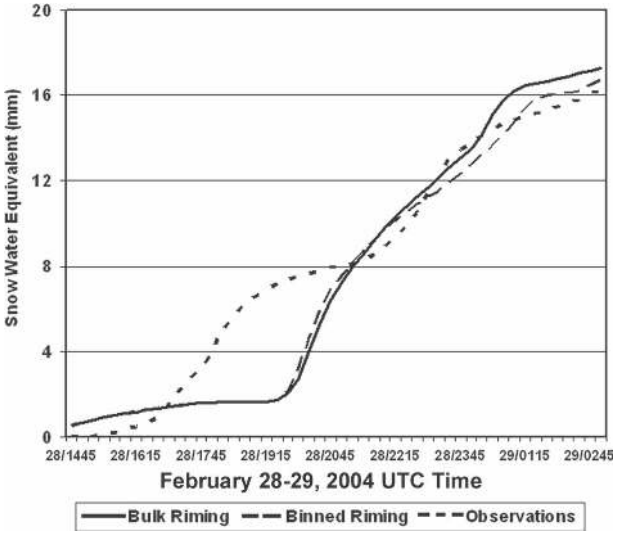


FIG. 6. Time series of accumulated snow-water equivalent (mm) from observations at SPL and from RAMS simulations using the bin and bulk riming approaches.

small, the difference in cloud water between the two simulations is very minimal. This relationship implies that other microphysical processes did not substantially contribute to the differences in cloud water in these simulations. The impact of variable riming upon precipitation is shown in Fig. 6 as a comparison between the time series of snow-water equivalent from observations near SPL and the model-closest grid point to SPL from the bin and bulk riming simulations. From the figure, the simulation using binned riming resulted in somewhat less accumulation and agrees more closely to the observations by the end of the simulations. These results suggest that use of a single value for collection efficiency that is based solely on the mean mass of the distribution tends to overpredict the amount of riming, and consequently, the accumulated precipitation in regions of heavy riming.

The impact of riming may also potentially feed back to the local dynamics via variations in latent heating resulting from phase changes (freezing–melting), vapor deposition, and evaporation. As such, Fig. 7 depicts time series of temperature, relative humidity, and horizontal and vertical wind speeds from the RAMS simulations, as well as SPL observations. The time series reveal relatively small variations between the simulations using the bulk and binned riming schemes. As would be expected, the largest variability occurs following saturation (100% RH) when the orographic cloud has formed and riming begins. The greatest variability is seen in the horizontal and vertical wind speeds, though the simulations generally agree within 1 m $s^{-1}$ for the horizontal winds and within 10 cm $s^{-1}$ for the

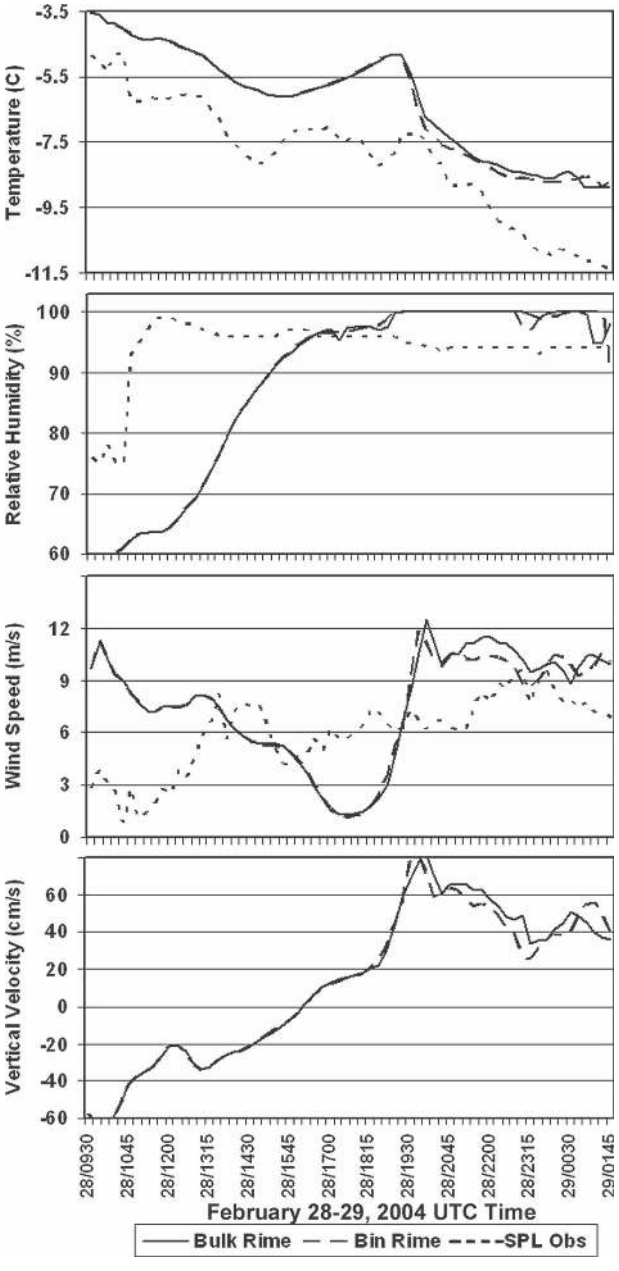


FIG. 7. Time series of meteorological fields comparing the model closest grid point to SPL from the binned and bulk riming method simulations and from SPL observations where available.

vertical wind speed. Furthermore, there is no discernable, consistent upward or downward bias in the time series of the winds when comparing the two simulations. Despite the relatively large changes in riming, the feedback to the local dynamics and thermodynamics is rather small, and it is most likely that local changes in the orographic cloud would be due to variations in the microphysics rather than variability in dynamics between simulations.

A comparison between the simulations and cloud-droplet characteristics measured at SPL provides further insight into the impact of the binned riming scheme. Figure 8 displays comparative time series of the cloud mixing ratio, mean droplet diameter, and droplet concentration. Model results are taken from the lowest model level and from the grid cell closest to the laboratory. The binned riming scheme impacted the total cloud liquid water content (LWC) by increasing the maximum value and sustaining this higher LWC for the duration of the orographic cloud event. The higher LWC more closely agrees with the maximum observed value from the FSSP. The simulated droplet mean diameter in the binned riming case responded with sizes that are consistently greater than in the bulk riming case; this was also in better agreement with mean diameters measured by the FSSP. There is greater variability between the two cases in the traces of droplet number concentration, with the bulk riming case producing a couple of spikes in the concentration that do not correspond with observations. The maximum value of the number concentration during the simulated cloud event with binned riming does match more closely with the observations and produces fewer deviations from the observed counts.

The impact of the binned riming scheme can be further examined through vertical cross sections of the simulated orographic cloud enshrouding Mt. Werner and SPL. Figure 9 displays west-to-east vertical cross sections of the hydrometeor mixing ratio spanning the slopes adjacent to SPL. The time chosen for this figure is near the time of the maximum observed cloud LWC at SPL, just following the onset of a period of heavy snowfall (2100 UTC February 28). Regardless of the riming scheme in use, an orographic cloud is produced predominantly on the western upslope side of the mountain, while subsidence leads to evaporative dissipation on the leeward slope. The maximum LWC is just upstream of the summit and SPL. The simulation using the binned riming scheme (Fig. 9b) contains a larger orographic cloud with higher values of cloud mixing ratio. Upon closer examination, the snow mixing ratio near the mountaintop and downwind of the orographic cloud experiences a slight reduction in the binned riming case due to the reduction in riming efficiency. Furthermore, what is most noticeable between the two cross sections is the disappearance of graupel near the mountaintop in the binned riming case. In such an environment, when riming efficiencies are high, as in the bulk riming case, the snowflakes begin to rime heavily. Some of them become water coated and are treated as graupel thereafter. The overestimated riming efficiencies of graupel in the bulk method expediently contribute to further riming, and they leave behind a more depleted cloud. The authors had suspected that graupel was a prime contributor to unrealistic depletion of cloud water via riming; it appears that this suspicion

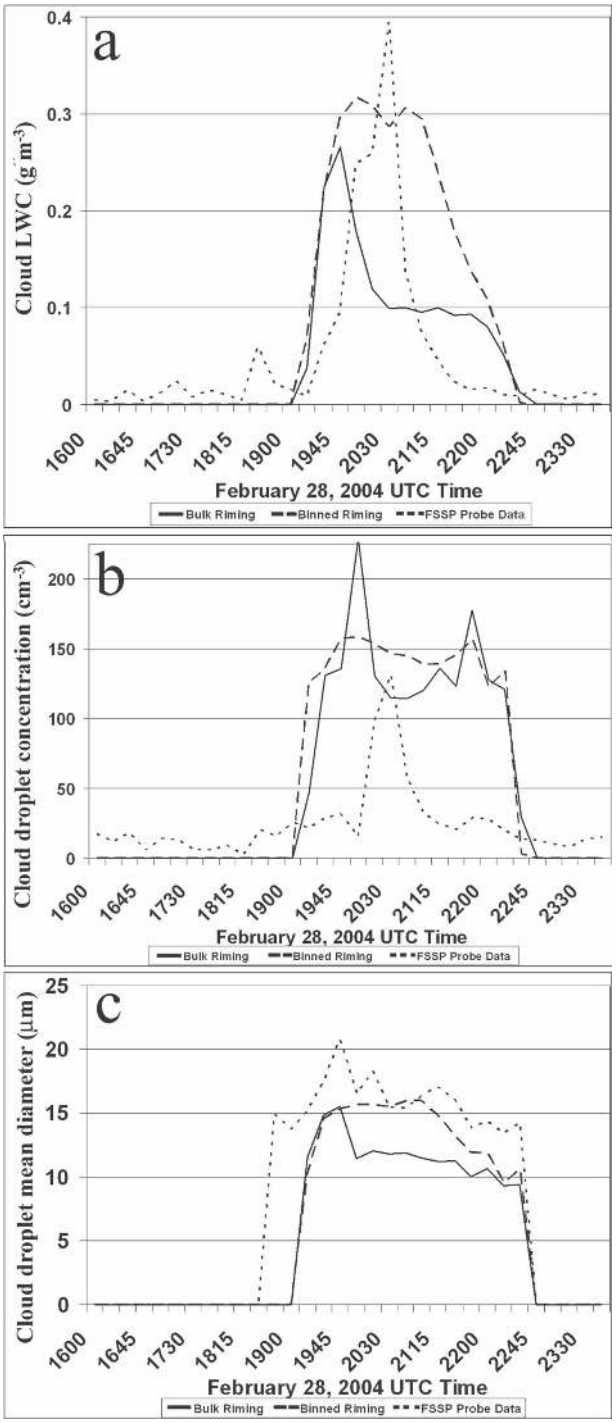


FIG. 8. RAMS vs observations at SPL for (a) cloud LWC (g $m^{-3}$), (b) cloud-droplet number concentration ($cm^{-3}$), and (c) cloud-droplet mean diameter ($\mu$m). Note that the RAMS grid point closest to SPL was used for comparison.

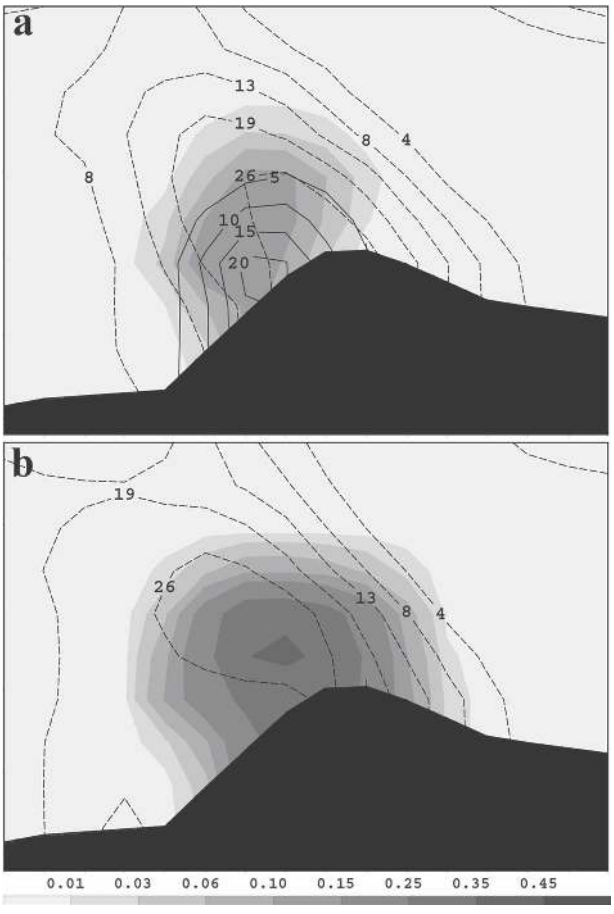


FIG. 9. West-to-east cross sections of hydrometeor mixing ratios centered on SPL at 2100 UTC 28 Feb 2004, near the time of maximum cloud LWC. Mixing ratios are of cloud water (g $kg^{-1}$, shaded), snow (g $kg^{-1} \times 100$, dashed lines), and graupel (g $kg^{-1} \times 100$, solid lines). The (a) bulk riming and (b) binned riming approaches were used.

was warranted and that the more realistic binned scheme tends to alleviate this bias where the seeder–feeder process is of importance.

## 5. Summary

The RAMS bulk microphysics module has been the focus of a development project to introduce an advanced bin model method to simulate the riming process within mixed-phase clouds. It had been suspected by the authors that the parameterized riming process in the bulk microphysics was overriming cloud water in mixed-phase clouds, thereby underpredicting supercooled cloud water amounts in wintertime events (Cotton et al. 2006). The primary deficiency of the former riming scheme was its use of a single collection efficiency to represent the collision–coalescence process over full gamma size distributions of cloud and ice particles. The chosen collection efficiency was based upon the mean mass of the cloud-droplet distribution.

The binned riming scheme, however, decomposes the gamma distribution of hydrometeors into 36 mass-doubling bins and computes each possible size bin interaction using the moment of methods from Tzivion et al. (1987). Published collection efficiencies between cloud droplets and each of the ice species (snow, aggregates, graupel, and hail) were obtained from Cober and List (1993), Greenan and List (1995), and Wang and Ji (2000). Each bin interaction is assigned an individual collection efficiency for the given particle sizes and fall speeds so as to more accurately determine the likelihood of collection by the ice particles. Given the tremendous variability in collection efficiency between cloud droplets and ice particles across a size distribution, this is certainly a more precise method of representing the riming process.

A wintertime snowfall event over Colorado that occurred from 28 to 29 February 2004 was chosen as a test case for a comparison between the bulk and binned riming methods. This case was first examined by Saleeby and Cotton (2005) because of available data of cloud-droplet properties from SPL. The laboratory was enshrouded by an orographic cloud during portions of this event, and roughly 27 cm of snow fell during this time period. The coexistence of cloud water and snowfall led to substantial riming during this event. The innermost nested grid, with 2-km grid spacing, was examined to compare the differences between the bulk and bin methods. The following conclusions were drawn:

1) Use of the bin approach resulted in a domain-wide reduction in riming by snow and aggregates (ice-only species) and by graupel and hail (possible ice and liquid mix). The greatest variation between the two methods occurred during periods of the heaviest riming.
2) The domain total cloud water mass remained higher when using the bin method.
3) Comparisons between SPL gridpoint simulations and observations of cloud mixing ratio, number concentration, and mean diameter suggest that the bin method is generally more accurate.
4) Cross sections of hydrometeor mixing ratios, centered on SPL, revealed that the bin method resulted in more retained supercooled cloud water, a reduced snow mixing ratio, and greatly reduced graupel mixing ratio. The reduction in graupel is due to minimizing the wet growth of any ice particle that occurs during periods of heavy riming.

While the use of a bulk microphysics collision–coalescence scheme provides a reasonable representation

of the riming process, the use of a single collection efficiency lacks the accuracy to truly simulate riming, especially when cloud liquid water content is high. Use of the binned approach, with collection kernel lookup tables, is still computationally efficient and provides for more realistically simulated riming growth of ice particles.

*Acknowledgments.* This research was supported by the National Science Foundation under Grant ATM-0451439. Logistical assistance from the Steamboat Ski and Resort Corporation is greatly appreciated. The Desert Research Institute is an equal opportunity service provider and employer and is a permittee of the Medicine Bow and Routt National Forests.

## REFERENCES

Borys, R. D., and M. A. Wetzel, 1997: Storm Peak Laboratory: A research, teaching and service facility for the atmospheric sciences. *Bull. Amer. Meteor. Soc.,* **78,** 2115–2123.

——, D. H. Lowenthal, and D. L. Mitchell, 2000: The relationships among cloud microphysics, chemistry, and precipitation rate in cold mountain clouds. *Atmos. Environ.,* **34,** 2593–2602.

——, ——, S. A. Cohn, and W. O. J. Brown, 2003: Mountaintop and radar measurements of anthropogenic aerosol effects on snow growth and snowfall rate. *Geophys. Res. Lett.,* **30,** 1538, doi:10.1029/2002GL016855.

Cober, S. G., and R. List, 1993: Measurements of the heat and mass transfer parameters characterizing conical graupel growth. *J. Atmos. Sci.,* **50,** 1591–1609.

Cotton, W. R., G. Thompson, and P. W. Mielke Jr., 1994: Real-time mesoscale prediction on workstations. *Bull. Amer. Meteor. Soc.,* **75,** 349–362.

——, and Coauthors, 2003: RAMS 2001: Current status and future directions. *Meteor. Atmos. Phys.,* **82,** 5–29.

——, R. McAnelly, G. Carrió, P. Mielke, and C. Hartzell, 2006: Simulations of snowpack augmentation in the Colorado Rocky Mountains. *J. Wea. Mod.,* **38,** 58–65.

Greenan, B. J. W., and R. List, 1995: Experimental closure of the heat and mass transfer theory of spheroidal hailstones. *J. Atmos. Sci.,* **52,** 3797–3815.

Harrington, J. Y., 1997: The effects of radiative and microphysical processes on simulated warm and transition season Arctic stratus. Ph.D. dissertation, Colorado State University, Atmospheric Science Paper 637, 289 pp.

Heggli, M. F., and R. M. Rauber, 1988: The characteristics and evolution of supercooled water in wintertime storms over the Sierra Nevada: A summary of microwave radiometric measurements taken during the Sierra Cooperative Pilot Project. *J. Appl. Meteor.,* **27,** 989–1015.

Hindman, E. E., 1986: Characteristics of supercooled liquid water in clouds at mountaintops in the Colorado Rockies. *J. Climate Appl. Meteor.,* **25,** 1271–1279.

Hobbs, P. V., M. K. Politovich, and L. F. Radke, 1980: The structures of summer convective clouds in eastern Montana. I: Natural clouds. *J. Appl. Meteor.,* **19,** 645–663.

Kain, J. S., and J. M. Fritsch, 1993: Convective parameterization for mesoscale models: The Kain–Fritsch scheme. *The Representation of Cumulus Convection in Numerical Models, Meteor. Monogr.,* No. 46, Amer. Meteor. Soc., 165–170.

Lew, J. K., D. C. Montague, H. R. Pruppacher, and R. M. Rasmussen, 1986a: A wind tunnel investigation on the riming of snowflakes. Part I: Porous disks and large stellars. *J. Atmos. Sci.,* **43,** 2392–2409.

——, ——, ——, and ——, 1986b: A wind tunnel investigation on the riming of snowflakes. Part II: Natural and synthetic aggregates. *J. Atmos. Sci.,* **43,** 2410–2417.

McAnelly, R. L., M. P. Meyers, E. M. Page, and W. R. Cotton, 2000: Application of a mesoscale model to fire weather forecasting. Postprints, *Second Southwest Weather Symp.,* Tucson, AZ, National Weather Service, 6 pp.

Meyers, M. P., R. L. Walko, J. Y. Harrington, and W. R. Cotton, 1997: New RAMS cloud microphysics parameterization. Part II. The two-moment scheme. *Atmos. Res.,* **45,** 3–39.

——, J. S. Snook, D. A. Wesley, and G. S. Poulos, 2003: A Rocky Mountain storm. Part II: The forest blowdown over the west slope of the northern Colorado mountains—observations, analysis, and modeling. *Wea. Forecasting,* **18,** 662–674.

Mitchell, D. L., R. Zhang, and R. L. Pitter, 1990: Mass-dimensional relationships for ice particles and the influence of riming on snowfall rates. *J. Appl. Meteor.,* **29,** 153–163.

Poulos, G. S., D. A. Wesley, J. S. Snook, and M. P. Meyers, 2002: A Rocky Mountain storm. Part I: The blizzard—Kinematic evolution and the potential for high-resolution numerical forecasting of snowfall. *Wea. Forecasting,* **17,** 955–970.

Rauber, R. M., and L. O. Grant, 1986: The characteristics and distribution of cloud water over the mountains of northern Colorado during wintertime storms. Part II: Spatial distribution and microphysical characteristics. *J. Climate Appl. Meteor.,* **25,** 489–504.

——, ——, D. Feng, and J. B. Snider, 1986: The characteristics and distribution of cloud water over the mountains of northern Colorado during wintertime storms. Part I: Temporal variations. *J. Climate Appl. Meteor.,* **25,** 468–488.

Reinking, R. F., J. B. Snider, and J. L. Coen, 2000: Influences of storm-embedded orographic gravity waves on cloud liquid water and precipitation. *J. Appl. Meteor.,* **39,** 733–759.

Saleeby, S. M., and W. R. Cotton, 2004: A large-droplet mode and prognostic number concentration of cloud droplets in the Colorado State University Regional Atmospheric Modeling System (RAMS). Part I: Module descriptions and supercell test simulations. *J. Appl. Meteor.,* **43,** 182–195.

——, and ——, 2005: A large-droplet mode and prognostic number concentration of cloud droplets in the Colorado State University Regional Atmospheric Modeling System (RAMS). Part II: Sensitivity to a Colorado winter snowfall event. *J. Appl. Meteor.,* **44,** 1912–1929.

Tzivion, S., G. Feingold, and Z. Levin, 1987: An efficient numerical solution to the stochastic collection equation. *J. Atmos. Sci.,* **44,** 3139–3149.

Verlinde, J., P. J. Flatau, and W. R. Cotton, 1990: Analytical solutions to the collection growth equation: Comparison with approximate methods and application to cloud microphysics parameterization schemes. *J. Atmos. Sci.,* **47,** 2871–2880.

Walko, R. L., W. R. Cotton, M. P. Meyers, and J. Y. Harrington, 1995: New RAMS cloud microphysics parameterization. Part I: The single-moment scheme. *Atmos. Res.,* **38,** 29–62.

Wang, P. K., and W. Ji, 2000: Collision efficiencies of ice crystals at low–intermediate Reynolds numbers colliding with supercooled cloud droplets: A numerical study. *J. Atmos. Sci.,* **57,** 1001–1009.

Warburton, J. A., and T. P. DeFelice, 1986: Oxygen isotopic composition of central Sierra Nevada precipitation. I: Identification of ice-phase water capture regions in winter storms. *Atmos. Res.,* **20,** 11–22.